# Multi-channel surface acoustic wave device and its application on all-fiber acousto-optic modulation

**Luming Zhao (赵路明)[1*] and Qida Zhao (赵启大)[2]**

[1] *Institute of Physics, Nankai University, Tianjin 300071, China*

[2] *Institute of Modern Optics, Nankai University, Tianjin 300071, China*

[*] *E-mail: Lumingzhao@hotmail.com*

Received February 18, 2009

The interaction of multi-channel surface acoustic waves (SAWs) and a guided optical wave in fiber is studied, and the corresponding coupled wave equations are derived. A novel two-channel SAW all-fiber acousto-optic modulator is designed, fabricated, and tested. The theoretical analysis is supported by the experimental results.

*OCIS codes:* 230.1040, 060.4080, 250.4110.

*doi: 10.3788/COL20100801.0107.*

All-fiber acousto-optic devices are important components in the field of fiber sensing, communication, and fiber laser[1−3]. The acousto-optic devices do not have to be inserted in a fiber system, so the insertion losses can be avoided. Several different types of all-fiber acousto-optic devices have been reported, including the acousto-optic devices using both surface and bulk acoustic waves[4], cylindrical transducer fabricated on fiber surface[5], and surface acoustic wave (SAW) sourced from piezoelectric transducer (PZT)[6,7], acoustic horn[8], and interdigital transducer (IDT)[9−11]. Most of all-fiber acousto-optic devices only have a single acoustical wave channel.

In this letter, the coupled wave equations of multi-channel SAWs and a guided optical wave (GOW) in fiber are derived. A novel all-fiber modulator of two-channel SAW device is fabricated. The SAWs of two channels have different center frequencies, and the GOW can be modulated by two SAWs simultaneously.

Let the incident GOW propagate along the $x$-axis. Its circular frequency and wave vector in the vacuum are denoted by $\omega$ and $\boldsymbol{k}$ respectively and the refraction index in the fiber medium is denoted by $\mu_0$. Let the circular frequency and wave vector of SAW of the $m$th channel be $\omega_m$ and $\boldsymbol{K_m}, (m = 1, 2, \cdots\cdots, N)$. The angle between the $x$-axis and wavefront of SAW of the $m$th channel is $\theta_m$. The geometry of two-channel acousto-optic interaction is shown in Fig.1.

In the fiber, the GOW is coupled with the multi-channel SAWs, and a series of polarization waves with compound frequencies are generated. The polarization waves generate optical radiations with these frequencies. The circular frequencies and wave vectors of polarization waves are[12,13]

$$\omega'_{(\overline{n})} = \omega + \sum_{m=1}^{N} n_m \omega_m, \tag{1}$$

$$\boldsymbol{K}'_{(\overline{n})} = \mu_0 \boldsymbol{k} + \sum_{m=1}^{N} n_m \boldsymbol{K}_m, \tag{2}$$

where $(\overline{n})$ represents $(n_1, n_2, \cdots, n_N)$, $n_m$ is the diffraction orders of the $m$th channel that may take any positive or negative integer values, i.e.,$n_m = 0, \pm 1, \pm 2, \cdots$.

The total field of the incident and diffracted optical beams can be represented by an expansion of planar waves:

$$\boldsymbol{E}(\boldsymbol{r}, t) = \exp(\mathrm{i}\omega t) \sum_{n_1=-\infty}^{\infty} \sum_{n_2=-\infty}^{\infty} \cdots \sum_{n_N=-\infty}^{\infty} \cdot \mathbf{e}_{(\overline{n})} E_{(\overline{n})}(z) \exp[\mathrm{i}(\omega'_{(\overline{n})} - \boldsymbol{K}'_{(\overline{n})} \cdot \boldsymbol{r})], \tag{3}$$

where $\mathbf{e}_{(\overline{n})}$ represents a unit vector of the electric field $\boldsymbol{E}_{(\overline{n})}$.

The strain tensor of multi-channel SAWs is

$$\boldsymbol{S}(\boldsymbol{r}, t) = \sum_{m=1}^{N} \boldsymbol{s}_m S_m \sin(\omega_m t - \boldsymbol{K}_m \cdot \boldsymbol{r}), \tag{4}$$

where $\boldsymbol{s}_m$ represents unit strain tensors introduced by SAW of the $m$th channel.

The acoustically-induced polarization generated by acousto-optic interaction is

$$\begin{aligned} \boldsymbol{P}(\boldsymbol{r}, t) &= \varepsilon_0 : \boldsymbol{X} : \boldsymbol{S}(\boldsymbol{r}, t) \cdot \boldsymbol{E}(\boldsymbol{r}, t) \\ &= (\varepsilon_0/2\mathrm{i}) \sum_{n_1=-\infty}^{\infty} \sum_{n_2=-\infty}^{\infty} \cdots \sum_{n_N=-\infty}^{\infty} \sum_{m=1}^{N} \\ &\quad \left\{ \left[ \boldsymbol{X} : \boldsymbol{s}_m \cdot \mathbf{e}_{(\overline{n}+\overline{a}_m)} S_m E_{(\overline{n}+\overline{a}_m)}(z) - \right. \right. \\ &\quad \left. \left. \boldsymbol{X} : \boldsymbol{s}_m \cdot \mathbf{e}_{(\overline{n}-\overline{a}_m)} S_m E_{(\overline{n}-\overline{a}_m)}(z) \right] \right\} \cdot \\ &\quad \exp[\mathrm{i}(\omega'_{(\overline{n})} t - \boldsymbol{K}'_{(\overline{n})} \cdot \boldsymbol{r})], \end{aligned} \tag{5}$$

where $\boldsymbol{X}$ is a nonlinear susceptibility tensor of medium, $(\overline{n} - \overline{a}_m)$ represents $(n_1, n_2, \cdots, n_{m-1}, n_m - 1, n_{m+1}, \cdots, n_{N-1}, n_N)$, and $(\overline{n} + \overline{a}_m)$ represents $(n_1, n_2, \cdots, n_{m-1}, n_m + 1, n_{m+1}, \cdots, n_{N-1}, n_N)$.

Substituting Eqs. (3) – (5) into Maxwell's equation

$$\nabla^2 \boldsymbol{E} - (1/c^2)\varepsilon \cdot \frac{\mathrm{d}^2}{\mathrm{d}t^2} \boldsymbol{E} = (1/c^2\varepsilon_0) \frac{\mathrm{d}^2}{\mathrm{d}t^2} \boldsymbol{P}, \tag{6}$$

and neglecting the second order terms, the coupled mode equations of GOW and multi-channel surface acoustic

 

waves are obtained as

$$\frac{\mathrm{d}}{\mathrm{d}z}E_{(\overline{n})}(z)-\mathrm{i}\Delta k_{(\overline{n})}E_{(\overline{n})}(z)=-\sum_{m=1}^{N}\frac{k_{(n)}^2}{4K'_{(n)z}}\cdot pS_m[\mu^2_{(\overline{n}+\overline{a}_m)}E_{(\overline{n}+\overline{a}_m)}-\mu^2_{(\overline{n}-\overline{a}_m)}E_{(\overline{n}-\overline{a}_m)}], \quad (7)$$

where $\Delta k_{(\overline{n})}$ is the phase mismatch per unit interaction length between the polarization wave vector $\boldsymbol{K}'_{(\overline{n})}$ and the diffracted optical wave vector $\boldsymbol{k}_{(\overline{n})}$, $p$ is the effective photoelastic coefficient.

In the normal acousto-optic interaction, $\mu_{(\bar{n}+\bar{a}_m)}=\mu_{(\bar{n}-\bar{a}_m)}=\mu_0$, Eq. (7) is reduced to[14]

$$\frac{\mathrm{d}}{\mathrm{d}z}E_{(\overline{n})}(z)-i\Delta k_{(\overline{n})}E_{(\overline{n})}(z)=-\sum_{m=1}^{N}\frac{k_{(n)}^2\mu_0^2}{4K'_{(n)z}}pS_m[E_{(\overline{n}+\overline{a}_m)}-E_{(\overline{n}-\overline{a}_m)}], \quad (8)$$

$$\Delta k_{(\overline{n})}=K'_{(\overline{n})z}-k_{(\overline{n})z}\cong\frac{(K'_{(\overline{n})})_z^2-(k_{(\overline{n})})_z^2}{2(K'_{(\overline{n})})_z}\cong\frac{{K'_{(\overline{n})}}^2-{k_{(\overline{n})}}^2}{2(K'_{(\overline{n})})_z}=\frac{\mu_0 k}{2b_{(\overline{n})}}\left\{1-\left(\frac{\mu_{(\overline{n})}}{\mu_0}\right)^2+\frac{2\sum_{m=1}^{N}n_mK_m}{\mu_0 k}\sin\theta_m+\left(\frac{\sum_{m=1}^{N}n_mK_m}{\mu_0 k}\right)^2\right\}, \quad (9)$$

where $b_{(\overline{n})}=K'_{(\overline{n})z}/\mu_0 k$.

The following normalized parameters are introduced to simplify the analysis[12]: $V_m=k\Delta\mu_m L_m/b_{(\overline{n})}$ is the normalized indexs of refraction modulation amplitude corresponding to $\Delta\mu_m$, where $\Delta\mu_m=-\frac{1}{2}\mu_0^3pS_m$ is the amplitude of the refractive index due to the acoustic signals of the $m$th channel, $L_m$ is the length of acousto-optic interaction, i.e., acoustic beam width of the $m$th channel; $Q_m=\overline{K}^2L_m/\mu_0 k\cos\theta_m$ indicates the mismatch of acousto-optic interaction; $\alpha=-\mu_0 k\sin\theta_m/\overline{K}$ describes the incidence angle of the light on the acoustic fields; $\beta_m=(K_m\cos\theta_m-\overline{K})/\overline{K}$ is the fractional deviation of acoustic signal wave number $K_m$ from the mid-band wave number $\overline{K}$; $G=\sum_{m=1}^{N}n_m$ is the diffraction order index.

Introducing the normalized parameters, the coupled mode Eqs. (8) and (9) take the form

$$\frac{\mathrm{d}}{\mathrm{d}z}E_{(\overline{n})}(z)-\mathrm{i}\Delta k_{(\overline{n})}E_{(\overline{n})}(z)=\sum_{m=1}^{N}\frac{V_m}{2L_m}[E_{(\overline{n}+\overline{a}_m)}(z)-E_{(\overline{n}-\overline{a}_m)}(z)], \quad (10)$$

$$\Delta k_{(\overline{n})}=\frac{Q_m}{2L_m}\left[\frac{2\mu_0 k}{\overline{K}^2}\sum_{m=1}^{N}n_mk_m\sin\theta_m+\left(G+\sum_{m=1}^{N}n_m\beta_m\right)\left(G+\sum_{m=1}^{N}n_m\beta_m-2\alpha\right)\right]. \quad (11)$$

In the Bragg regime ($Q>4\pi$), phase mismatch can only be minimized for the zeroth and first diffraction orders ($G=0,\pm1$). For Bragg incidence $\alpha\cong1/2$, $\sum_{m=1}^{N}n_m\beta_m\ll1$ and $\theta_m$ is very small. Equations (10) and (11) take the forms

$$\frac{\mathrm{d}}{\mathrm{d}z}E^0_{(\bar{n})}(z)=\sum_{m=1}^{N}\frac{V_m}{2L_m}E^1_{(\bar{n}+\bar{a}_m)}(z), \quad (12)$$

$$\frac{\mathrm{d}}{\mathrm{d}z}E^1_{(\bar{n})}(z)=-\sum_{m=1}^{N}\frac{V_m}{2L_m}E^0_{(\bar{n}-\bar{a}_m)}(z), \quad (13)$$

where $E^G_{(\bar{n})}$ is the amplitude, the superscript $G$ indicates the diffracted order of the mode $(\overline{n})$.

Under the initial conditions, $E_{(\bar{n})}=E_0,(\bar{n})=(\bar{0})$ and $E_{(\bar{n})}=0,(\bar{n})\neq(\bar{0})$, only when the first order diffracted beam is presence in the $m$th channel, the solutions of Eqs. (12) and (13) are[12–15]

$$\eta^1_m=|E^1_m(L_m)|^2/|E^0_m(L_m(0))|^2=(V_m/2\sigma_m)^2\sin^2\sigma_m, \quad (14)$$

where $L_m(0)$ denotes the starting point of interaction in the $m$th channel, $\eta^1_{(\bar{n})}$ denotes the diffraction efficiencies, and

$$\sigma_m=[\zeta_m^2+(V_m/2)^2]^{1/2}=(1/4)\{[Q_m(1-2\alpha_m)]^2+4V_m^2\}^{1/2}, \quad (15)$$

$$\zeta_m=Q_m(2\alpha_m-1)/4. \quad (16)$$

In the above normalized parameter expressions,$V_m$can be replaced by the acoustic power entering in fiber of the $m$th channel $P_{am}$. $V_m$ is given according to the relation of acoustic power $P_m$, strain $S_m$, and $P_{am}$ as[16,17]

$$V_m=\frac{\pi}{\lambda_0\cos\theta_m}\left(\frac{2M_2L_mP_{am}}{H_m}\right)^{1/2}|F|, \quad (17)$$

where $\lambda_0$ is the free space optical wavelength, $H_m$ is the depth of the SAW, and $M_2$ is the acousto-optic figure of merit of material related to the velocity of SAW $V_a$ and the density of the material $\rho$.

For precise Bragg incidence $\alpha_m=1/2$, the first order diffraction efficiency of each channel can be obtained from Eqs. (14)–(17) as

$$\eta^1_m=\frac{|E^1_m(L_m)|^2}{|E^0_m(L_m(0))|^2}=\sin^2\left(\frac{V_m}{2}\right)=\sin^2\left[\frac{\pi}{\lambda\cos\theta_m}\left(\frac{M_2L_mP_{am}}{2H_m}\right)^{1/2}|F|\right], \quad (18)$$

where $F$ is the overlap integral, which includes the contributions of the acousto-optic ($F_{\mathrm{ao}}$), the electro-optic ($F_{\mathrm{eo}}$), and the surface ripple ($F_{\mathrm{sr}}$) effects, i.e.,

$$F=F_{\mathrm{ao}}+F_{\mathrm{eo}}+F_{\mathrm{sr}}. \quad (19)$$

The overlap integral occurs only for guided wave structures having a value from 0 to 1. It depends on the field distributions of the incident, diffracted optical waves, and the acoustic waves. For the bulk wave case, $F=1$, Eq. (19) is in agreement with the diffracted efficiency of SAW and GOV in thin-film guided wave structures[16–18].

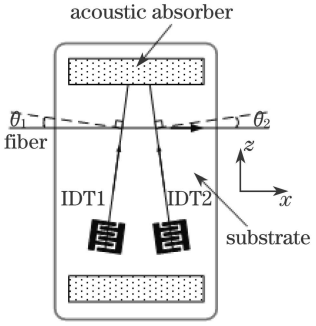


Fig. 1. Two-channel SAW all-fiber acousto-optic diffraction geometry.

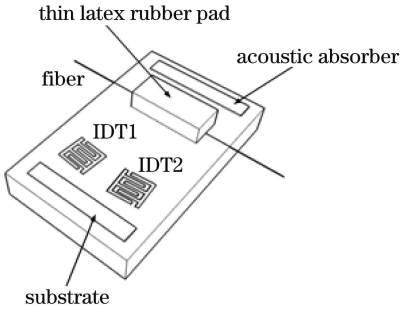


Fig. 2. Two-channel SAW all-fiber acousto-optic modulator.

In the multi-channel case, the SAWs which have different frequencies interact with the light beam. Every diffracted light beam will be re-diffracted by SAWs of subsequent channels, and the undiffracted light beams continue propagating along the fiber to output.

According to Eq. (18), the intensity of incident optical beam in the $m$th channel is

$$\begin{aligned}|E_m^0(L_m(0))|^2 &= |E_{m-1}^0(L_{m-1}(0))|^2 - |E_{m-1}^1(L_{m-1})|^2 \\ &= (1-\eta_{m-1}^1)|E_{m-1}^0(L_{m-1}(0))|^2 \\ &= (1-\eta_1^1)(1-\eta_2^1)\cdots(1-\eta_{m-1}^1)|E_0|^2 \\ &= \left[1-\sin^2\left(\frac{V_1}{2}\right)\right]\left[1-\sin^2\left(\frac{V_2}{2}\right)\right] \\ &\quad \cdots\left[1-\sin^2\left(\frac{V_{m-1}}{2}\right)\right]|E_0|^2 \\ &= \prod_{m=1}^{m-1}\left[1-\sin^2\left(\frac{V_m}{2}\right)\right]|E_0|^2, \end{aligned} \tag{20}$$

and the intensity of the first diffracted optical beam in this channel is

$$|E_m^1(L_m)|^2 = \eta_m^1|E_m^0(L_m(0))|^2 = \sin^2\left(\frac{V_m}{2}\right) \times \prod_{m=1}^{m-1}\left[1-\sin^2\left(\frac{V_m}{2}\right)\right]|E_0|^2. \tag{21}$$

This beam will be weakened because it is diffracted in the following channels, and the output intensity becomes

$$\begin{aligned}|E_m^1|^2 &= |E_m^1(L_m)|^2(1-\eta_{m+1}^1)(1-\eta_{m+2}^1)\cdot \\ &\quad \cdots(1-\eta_N^1)|E_0|^2 \\ &= \sin^2\left(\frac{V_m}{2}\right)\prod_{m=1}^{m-1}\left[1-\sin^2\left(\frac{V_m}{2}\right)\right] \\ &\quad \times\prod_{m=m+1}^{N}\left[1-\sin^2\left(\frac{V_m}{2}\right)\right]|E_0|^2 \\ &= \sin^2\left(\frac{V_m}{2}\right)\prod_{m'=1}^{N}\left[1-\sin^2\left(\frac{V_{m'}}{2}\right)\right]|E_0|^2 \end{aligned} \tag{22}$$

where $m'$ represents $1, 2, \cdots, m-1, m+1, \cdots, N-1, N$.

Neglecting the second order terms, the output optical beams are

$$A = \sum_{m=1}^{N} A_m \cos(\omega_m t), \tag{23}$$

where $A_m = |E_m^1|$.

We designed and fabricated two kinds of two-channel SAW devices for which the piezoelectric substrates are made of $LiNbO_3$ and quartz crystal, respectively. One of the devices is based on Y-cut $LiNbO_3$ substrate with center frequencies 50 and 100 MHz, respectively. The interaction geometry is shown in Fig. 1.

The SAWs generated by IDTs propagate on the $xz$ plane along the $z$-axis and the wavefronts are making the angles of $\theta_1$ and $\theta_2$ from the $x$-axis respectively. A single mode optical fiber is pressed onto the surface of substrate with a thin rubber pad, and an incident GOW in fiber propagates on the $xz$ plane along the $x$-axis. The angles of optical wave and SAWs correspond to the Bragg diffracted condition at two different acoustic frequencies, respectively. The schematic structure diagram of two-channel acousto-optic device is shown in Fig. 2.

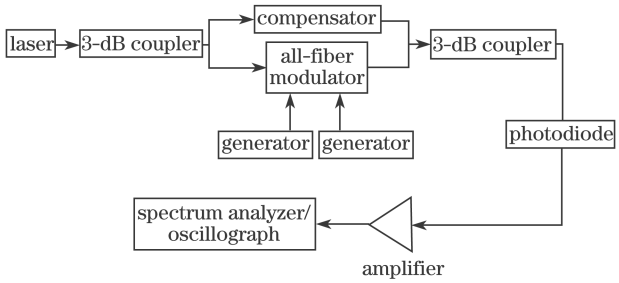


Fig. 3. Experimental setup.

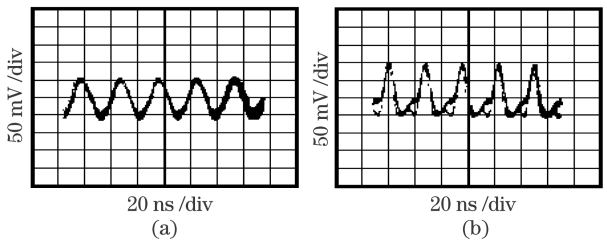


Fig. 4. Output waveforms of all-fiber acousto-optic modulator. Driving frequency is 50 MHz. Driving electric power: (a) $P_{a1} = 0.6$ W, $P_{a2} = 0.07$ W; (b) $P_{a1} = P_{a2} = 0.6$ W.

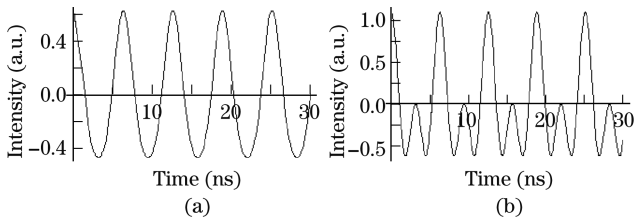


Fig. 5. Simulation curves of all-fiber acousto-optic modulator. (a) $P_{a1}=0.6$ W, $P_{a2}=0.07$ W; (b) $P_{a1}=P_{a2}=0.6$ W.

A 1.55-$\mu$m laser was utilized as the light source. The incident light in fiber was split by a 3-dB coupler. The two beams propagated through the two arms of a Mach-Zehnder interferometer, the all-fiber modulator was placed in one arm and a compensator of optical path in the other arm. Passing the second 3-dB coupler, the light entered the measurement system, which consisted photodiode, amplifier, spectrum analyzer, and oscillograph. A schematic diagram of the experimental setup is shown in Fig. 3.

The main parameters of two-channel device used in the experiment areas follows: $L_m=100\lambda_a$, where $\lambda_a$ is the acoustic wavelength, $V_a=3485$ m/s, $M_2=6.95\times10^{-15}$ s$^3$/kg, $H_m=\lambda_a$, the center frequencies of the channels 1 and 2 are 50 and 100 MHz, respectively. The output waveforms modulated by SAW in the channel 1 is shown in Fig. 4. Figure 4(a) is the output waveform driven by the acoustic power whose value is 0.6 W at channel 1 and 0.07 W at channel 2. Figure 4(b) is the waveform driven by 0.6 W at two channels. If the difference between the driving powers is smaller, the crosstalk between two channels will be more intense.

The signal modulated by acoustic wave with frequency of 50 MHz in channel 1 is disturbed by acoustic wave with frequency of 100 MHz in channel 2. Therefore, Eq. (23) becomes

$$A=A_1\cos(2\pi f_1 t)+A_2\cos(2\pi f_2 t), \tag{24}$$

where

$$A_1=\left\{\sin^2\left(\frac{V_1}{2}\right)\left[1-\sin^2\left(\frac{V_2}{2}\right)\right]\right\}^{1/2}|E_0|,$$

$$A_2=\left\{\sin^2\left(\frac{V_2}{2}\right)\left[1-\sin^2\left(\frac{V_1}{2}\right)\right]\right\}^{1/2}|E_0|.$$

Theoretical output waveforms of the two-channel modulator, simulated under the above experimental parameters, are illustrated in Fig. 5. Figure 5(a) is the waveform taken $P_{a1}=0.6$ W and $P_{a2}=0.07$ W. Figure 5(b) is the waveform taken by $P_{a1}=P_{a2}=0.6$ W. When the difference between the driving powers becomes smaller, the values of $A_1$ and $A_2$ is closer, so the interference between the two channels will be more intense. Apparently, the theoretical calculation conforms well to the experimental results.

When the driving power values of the two channel are reversed, the signal modulated by acoustic wave with frequency 100 MHz in channel 2 is disturbed by the acoustic wave with frequency of 50 MHz in channel 1. The output waveform is also obtained. The experimental results and theoretical analyses are similar to those in the former case.

In conclusion, multi-channel acousto-optic GOW device can provide a very wide bandwidth[19] and accomplish multiple modulations of signals. The results of theory and experiments indicate multiple-channel SAW all-fiber acousto-optic modulator can modulate light beam using multiple channels simultaneously. The output principal diffraction intensity of a certain channel is weakened because the diffraction beam is re-diffracted in the following channels and its incident light is diffracted in the previous channels. When multi-channel SAWs interact with GOW, the driving power of one channel is obviously stronger than others, the modulation signal waveform can be obtained accurately; whereas the driving powers of channels have near magnitude, and the waveform of the output signal is distorted. The multi-channel SAW all-fiber modulator can be used in optical communication, optical sensors, and optical signal processing.

This work was supported by the National Natural Science Foundation of China (No. 60572018) and the Tianjin Science and Technology Developing Programs (Nos. 05YFGPGX04900 and 07ZCKFGX00200).

## References

1. S. Zhen, R. Liu, B. Yu, J. Zhang, and B. Han, Chin. Opt. Lett. **7,** 26 (2009).
2. J Ning, W. Zhang, L. Shang, G. Fan, Q. Han, and L. Zhou, Chinese J. Lasers (in Chinese) **35,** 483 (2008).
3. C. Gao, W. Zhao, Y. Wang, and S. Zhu, Chinese J. Lasers (in Chinese) **35,** 651 (2008).
4. W. P. Risk, R. C. Youngquist, G. S. Kino, and H. J. Shaw, Opt. Lett. **9,** 309 (1984).
5. M. P. Roe, B. Wacogne, and C. N. Pannell, IEEE Photon. Technol. Lett. **8,** 1026 (1996).
6. P. A. Greenhalgh, A. P. Foord, and P. A. Davies, Electron. Lett. **25,** 1206 (1989).
7. J. O. Askautrud and H. E. Engan, Opt. Lett. **15,** 649 (1990).
8. S. R. M. Carneiro, E. A. Castro, O. Lisbôa, and S. L. A. Carrara, Opt. Lett. **17,** 831 (1992).
9. D. B. Patterson, A. A. Godil, G. S. Kino, and B. T. Khuri-Yakub, Opt. Lett. **14,** 248 (1989).
10. W. P. Risk, G. S. Kino, and H. J. Shaw, Opt. Lett. **11,** 115 (1986).
11. B. Liao, Q. Zhao, and Y. Zhang, Opt. Commun. **242,** 361 (2004).
12. I. C. Chang, IEEE Trans. Sonics Ultrason. **23,** 2 (1976).
13. J. Xu and R. Stroud, *Acousto-Optic Devices: Principles, Design, and Applications* (Wiley, New York, 1992).
14. L. Zhao, Q. Zhao, L. Liu, and B. Liao, Proc. SPIE **5644,** 21 (2005).
15. D. L. Hecht, IEEE Trans. Sonics Ultrason. **24,** 7 (1977).
16. R. V. Schmidt, IEEE Trans. Sonics Ultrason. **23,** 22 (1976).
17. E. G. H. Lean, J. M. White, and C. D. W. Wilkinson, Proc. IEEE **64,** 779 (1976).
18. J. M. White, P. F. Heidrich, and E. G. Lean, Electron. Lett. **10,** 510 (1974).
19. C. S. Tsai, Le T. Nguyen, S. K. Yao, and M. A. Alhaider, Appl. Phys. Lett. **26,** 140 (1975).